Hepatic cholesterol crystals and crown-like structures distinguish NASH from simple steatosis[S]

George N. Ioannou,[1,*,†] W. Geoffrey Haigh,[*,†] David Thorning,[§] and Christopher Savard[*,†]

Research Enhancement Award Program* and Department of Pathology,[§] Veterans Affairs Puget Sound Health Care System, Seattle, WA; and Division of Gastroenterology,[†] Department of Medicine, University of Washington, Seattle, WA

Abstract **We sought to determine whether hepatic cholesterol crystals are present in patients or mice with nonalcoholic fatty liver disease/nonalcoholic steatohepatitis (NASH), and whether their presence or distribution correlates with the presence of NASH as compared with simple steatosis. We identified, by filipin staining, free cholesterol within hepatocyte lipid droplets in patients with NASH and in C57BL/6J mice that developed NASH following a high-fat high-cholesterol diet. Under polarized light these lipid droplets exhibited strong birefringence suggesting that some of the cholesterol was present in the form of crystals. Activated Kupffer cells aggregated around dead hepatocytes that included strongly birefringent cholesterol crystals, forming "crown-like structures" similar to those recently described in inflamed visceral adipose tissue. These Kupffer cells appeared to process the lipid of dead hepatocytes turning it into activated lipid-laden "foam cells" with numerous small cholesterol-containing droplets. In contrast, hepatocyte lipid droplets in patients and mice with simple steatosis did not exhibit cholesterol crystals and their Kupffer cells did not form crown-like structures or transform into foam cells. Our results suggest that cholesterol crystallization within hepatocyte lipid droplets and aggregation and activation of Kupffer cells in crown-like structures around such droplets represent an important, novel mechanism for progression of simple steatosis to NASH.**—Ioannou, G. N., W. G. Haigh, D. Thorning, and C. Savard. **Hepatic cholesterol crystals and crown-like structures distinguish NASH from simple steatosis.** ***J. Lipid Res.*** **2013.** 54: **1326–1334.**

Supplementary key words Kupffer cells • foam cells • steatohepatitis • nonalcoholic steatohepatitis

Nonalcoholic fatty liver disease (NAFLD), defined as increased lipid deposition within hepatocytes in the absence of viral hepatitis or excessive alcohol consumption, is extremely common affecting 15–46% of adults in the United States (1–3). However, the majority of patients with NAFLD have "simple steatosis" defined by hepatic steatosis in the absence of substantial inflammation or fibrosis. Such patients generally have a benign clinical course with a very low probability of developing progressive liver dysfunction and cirrhosis (4). In contrast, 10–30% of patients with NAFLD develop a more aggressive condition known as nonalcoholic steatohepatitis (NASH) (3), characterized by varying degrees of hepatic inflammation, balloon hepatocytes, and fibrosis in addition to hepatic steatosis. Steatohepatitis can progress to cirrhosis, liver failure, and hepatocellular carcinoma in a variable proportion of patients (4, 5).

It is clearly established that central obesity and insulin resistance are important risk factors for the development of hepatic steatosis. However, the factors responsible for the development of progressive steatohepatitis remain unclear. Determining these factors would: *i*) clarify the pathogenesis of progressive steatohepatitis; *ii*) help to distinguish the subgroup of patients with NAFLD who are likely to develop progressive NASH and cirrhosis; and *iii*) potentially point to targeted treatments.

Recent reports by our group and others suggest that dietary and hepatic cholesterol are critical factors in the development of steatohepatitis in animal models (6–9). Human studies also support the hypothesis that dietary cholesterol plays a role in the development of steatohepatitis. In a large nationally representative epidemiological study, we reported that dietary cholesterol consumption was independently associated with the development of cirrhosis (10). Finally, inhibition of intestinal cholesterol absorption by administration of ezetimibe to patients with NASH (11, 12) has been reported to improve hepatic inflammation and steatosis; these studies were not, however, randomized or controlled.

This work was supported by a grant from the Research Enhancement Award Program (to G.N.I.), Office of Research and Development, Veterans Affairs Puget Sound Health Care System, Seattle, WA. The authors report no conflicts of interest.

Manuscript received 11 December 2012 and in revised form 7 February 2013.

Published, JLR Papers in Press, February 7, 2013
DOI 10.1194/jlr.M034876

Abbreviations: H and E, hematoxylin and eosin; HF, high-fat; HFHC, high-fat high-cholesterol; NAFLD, nonalcoholic fatty liver disease; NAS, nonalcoholic fatty liver disease activity score; NASH, nonalcoholic steatohepatitis; TNFα, tumor necrosis factor α.

[1] To whom correspondence should be addressed.
e-mail: georgei@medicine.washington.edu

[S] The online version of this article (available at http://www.jlr.org) contains supplementary data in the form of four figures and one table.

Cholesterol, a naturally occurring molecule abundant in most tissues, has traditionally been viewed as inert. Recently, however, its crystalline form has been shown to induce inflammation by stimulating the NLRP3 inflammasome in animal models of atherosclerosis (13). We therefore hypothesized that cholesterol crystals may form in fatty livers, which are characterized by high concentrations of cholesterol as well as other lipids, and may be the hitherto unrecognized signal that leads to the progression from simple steatosis to progressive steatohepatitis. Cholesterol crystals have been described before in the livers of patients with cholesteryl ester storage disease (14), but not, to our knowledge, in patients with NAFLD/NASH.

We therefore aimed to determine whether cholesterol crystals are present in the livers of patients with NAFLD/NASH or in a mouse model of NAFLD/NASH. Additionally, we wanted to determine whether the presence or distribution of hepatic cholesterol crystals correlates with the presence of NASH and distinguishes it from simple steatosis.

METHODS

Patients with simple steatosis or steatohepatitis

From an existing human liver biorepository at Veterans Affairs Puget Sound Health Care System (VAPSHCS), we randomly selected 4 patients with histological NASH, defined as NAFLD activity score (NAS) of 5 or greater, with at least 1 point in each of the three components of the NAS score (steatosis 0–3, lobular inflammation 0–3, ballooning degeneration 0–2); and 3 patients with histological simple steatosis, defined as NAS score 2–3 with no ballooning degeneration (15). We retrieved liver tissue from these patients that had been flash frozen in liquid nitrogen immediately after liver biopsy. Fasting laboratory tests were prospectively performed just prior to liver biopsy as well as completion of questionnaires and collection of demographic and clinical information.

Mice with simple steatosis or steatohepatitis

Male C57BL/6J littermate mice were fed for 30 weeks either a high-fat (HF) (15%, w/w) diet with no cholesterol (n = 8) or a high-fat (15%) high-cholesterol (1%) (HFHC) diet (n = 8). The experimental diets were prepared by Bioserve (Frenchtown, NJ) and their composition is described in supplementary Table I. Mice were euthanized 30 weeks after initiation of the experimental diets by cervical dislocation following isoflurane anesthesia. We previously reported that mice fed a HF diet developed increased hepatic fat deposition with little inflammation and no fibrosis (simple steatosis) (16). Mice on a HFHC diet developed significantly more profound hepatic steatosis, substantial inflammation, and perisinusoidal fibrosis (steatohepatitis), associated with adipose tissue inflammation and a reduction in plasma adiponectin levels (16).

Hepatic histology

Formalin-fixed liver sections. Human and mouse formalin-fixed paraffin-embedded liver tissue was sectioned and stained with hematoxylin and eosin (H and E) and with Masson's trichrome or Sirius red (for collagen). Histological steatosis, inflammation, and fibrosis were assessed semiquantitatively by a "blinded" liver pathologist according to the scoring system proposed by Kleiner et al. (15).

Frozen liver sections. Human liver biopsies were placed in cryovials and frozen in liquid nitrogen immediately after liver biopsy. Just prior to cutting, the frozen human livers were embedded in optimal cutting temperature (OCT) compound and frozen on dry ice. Mouse liver portions were embedded in OCT and frozen in liquid nitrogen immediately after removal. Frozen sections (10 μM in thickness) were allowed to come to room temperature, immediately coverslipped using pure glycerol as the mounting medium without applying any stain, and examined using a Nikon Eclipse microscope with or without a polarizing filter, to evaluate for the presence of birefringent crystals.

Staining for unesterified "free" cholesterol. Frozen liver sections were stained with filipin, which identifies free cholesterol by interacting with its 3β-hydroxy group (17), as follows. After fixing for 15 min in formalin, liver sections were washed with phosphate buffered saline (PBS), and then treated with 10% fetal bovine serum (FBS) in PBS for 30 min. Filipin (Sigma Chemical Co., St. Louis, MO) was dissolved in a small volume of dimethylsulfoxide then diluted to 0.25 mg/ml in 10% FBS/PBS and added to the tissue for 1 h at room temperature. Slides were washed with 10% FBS/PBS once and PBS twice. Slides were coverslipped using Aquamount (Lerner, Pittsburgh, PA) and examined using a fluorescent Nikon Eclipse microscope with an excitation 340-380/emission 435-485 filter in place.

Staining for macrophages. Frozen mouse and human sections were stained with anti-CD68 antibodies, which identify macrophages (including hepatic Kupffer cells), followed by secondary antibodies labeled with Alexa Fluor 488 (Invitrogen, Camarillo, CA) and then examined using a fluorescent microscope. To determine whether macrophages were activated, mouse liver sections were also stained with rat anti-mouse CD11b (also known as macrophage-1 antigen or Mac-1) antibodies identified by a goat anti-rat secondary antibody linked to horseradish peroxidase or with anti-tumor necrosis factor α (TNFα) antibodies identified by secondary antibodies labeled with Alexa Fluor 488. We will henceforth use the term "Kupffer cells" (resident tissue macrophages of the liver) to describe CD68-positive cells, while acknowledging that some of these cells may be macrophages recruited from the circulation.

Electron microscopy

At time of tissue removal, pieces of mouse or human liver were fixed in Trump's fixative. After postfixation in osmium tetroxide, the samples were embedded in epoxy resin and thinly sliced (0.12 μM). The sections were stained with a solution of uranyl acetate followed by aqueous lead citrate and viewed using a JEOL (Tokyo, Japan) transmission electron microscope. Thicker sections (1 μM) of the embedded tissue that had been fixed in osmium tetroxide were counterstained with methylene blue and viewed under a regular light microscope. Osmium tetroxide binds at the carbon-carbon double bonds of unsaturated fatty acids, and therefore could potentially distinguish lipid droplets that contained only free cholesterol (no staining with osmium) from lipid droplets that contained triglycerides or cholesterol esters.

Hepatic lipid analysis

Lipids were extracted from frozen mouse liver using the Folch method (18). The neutral lipid fractions were prepared by solid phase extraction on Bond Elut Si cartridges (Varian Corp.,

Walnut Creek, CA) and the triglycerides, diglycerides, cholesterol esters, and free cholesterol were then separated and quantified by normal phase HPLC/ELSD. Free fatty acids were esterified by boron trifluoride/methanol and the methyl esters were then separated by GC, using a 60 m HP-Innowax capillary column (Agilent Technologies, Santa Clara, CA). Insufficient frozen human liver tissue was available to perform hepatic lipid analysis.

Hepatic mRNA analysis

Total RNA was isolated from mouse liver tissue using RNeasy minicolumns (Qiagen, Valencia, CA) and reverse transcribed to cDNA. Quantitative real-time RT-PCR was performed using the ABI 7500 sequence detection system (Applied Biosystems, Foster City, CA) with β-actin as the housekeeping gene. The hepatic gene expression levels of 4 genes related to the NLRP3 inflammasome were assessed [Nalp3, ASC (apoptosis-associated speck-like caspase recruitment domain containing protein), Caspase-1, and Pannexin-1] (19) because cholesterol crystals have been shown to induce inflammation by stimulating the NLRP3 inflammasome in animal models of atherosclerosis (13). Gene expression studies were only performed on mouse liver tissue.

Institutional approvals

All experimental procedures were undertaken with approval from the Institutional Review Board and the Institutional Animal Care and Use Committee of the Veterans Affairs Puget Sound Health Care System. Human subjects provided informed consent for participation in our biorepository. Animal investigations conformed to the Public Health Policy on Humane Care and Use of Laboratory Animals.

RESULTS

All patients with NASH (n = 4) or simple steatosis (n = 3) were obese males with mildly elevated serum ALT level and normal serum bilirubin level (**Table 1**). All patients with NASH had diabetes mellitus while only one of three patients with simple steatosis had diabetes.

Mice fed a HFHC diet developed steatohepatitis and had higher body weight and liver weight; higher hepatic triglyceride, diglyceride, cholesterol ester, and free cholesterol concentration; higher plasma ALT, cholesterol, and insulin levels; and lower serum adiponectin levels than mice fed a HF diet which developed simple steatosis (**Table 2**).

Light microscopy of formalin-fixed human and mouse liver sections stained with H and E, Sirius red, and Masson's trichrome confirmed the presence of lobular inflammation, steatosis, and perisinusoidal fibrosis in specimens with steatohepatitis, and the absence of substantial inflammation or fibrosis in those with simple steatosis (**Fig. 1**).

Examination under polarized light of frozen liver sections from humans and mice (**Fig. 2**) with steatohepatitis revealed strongly birefringent crystals within a large proportion of hepatocyte lipid droplets. Those droplets with birefringence also stained prominently with filipin, suggesting that the birefringence was due to cholesterol crystals. In both species, livers with only simple steatosis showed neither birefringence nor filipin staining in steatotic hepatocytes.

CD68-positive cells (Kupffer cells) formed "crown-like" aggregates only around hepatocytes which contained clearly birefringent lipid droplets (**Figs. 3, 4**, and supplementary Fig. I), most notably around mouse hepatocytes containing the most strongly birefringent lipid droplets, which appeared as "Maltese crosses" under polarized light (Fig. 4B, D). Moreover, the Kupffer cells that surrounded hepatocytes with birefringent lipid droplets, stained intensely with filipin (Fig. 3), indicating that they contained free cholesterol, and for CD11b and TNFα (Fig. 4E, F) suggesting that they were activated. These findings were observed both in mice and humans with NASH, although the Kupffer cells appeared more slender in the human livers (Fig. 3A, B and supplementary Fig. III). Taken together, these findings suggest that in NASH, Kupffer cells aggregate around hepatocytes that contain cholesterol crystals, accumulate cholesterol, and become activated.

The osmium and methylene blue stained sections as well as the electron micrographs demonstrated that the aggregates of Kupffer cells actually occurred around the remnant lipid droplets of dead hepatocytes (marked by asterisks in **Fig. 5** and supplementary Fig. II). In many instances, the Kupffer cells directly abutted on lipid cores without evident hepatocyte cytoplasm (Fig. 5D and supplementary Fig. IID, E, H).This created crown-like structures identical to those recently described in inflamed visceral adipose tissue (20, 21). While normal lipid droplets

TABLE 1. Characteristics of patients with simple steatosis versus NASH

	Simple Steatosis			NASH			
Patient number	1	2	3	4	5	6	7
Steatosis (0–3)	1	2	2	2	3	2	1
Inflammation (0–3)	1	1	1	2	1	2	2
Ballooning (0–2)	0	0	0	1	2	2	2
Fibrosis (0–4)	0	0	0	1A	1A	2	3
Age	37	60	62	44	41	45	61
Gender	Male	Male	Male	Male	Male	Male	Male
Race	White	White	White	Black	White	White	White
Diabetes	No	Yes	No	Yes	Yes	Yes	Yes
Body mass index (Kg/m^2)	30	32	31	36	44	35	36
Plasma or serum levels, fasting							
ALT (U/L)	74	61	44	78	83	67	104
Bilirubin (mg/dl)	0.5	0.2	0.3	0.3	0.6	0.6	0.4
Insulin (μU/ml)	16	13	22	40	59	96	133
Glucose (mg/dl)	85	109	102	143	127	273	104
Hemoglobin A 1c (%)	5.2	7.0	5.4	7.0	7.1	7.9	7.6

TABLE 2. Characteristics (mean ± SD) of mice fed a HF diet (simple steatosis) versus mice fed a HFHC diet (NASH) for 30 weeks

	HF Diet Simple Steatosis (N = 8)	HFHC Diet NASH (N = 8)
Body weight (g)	36.3 ± 4.9	39.9 ± 3.8*
Body weight gain (%)	13 ± 4	32 ± 7*
Liver weight (g)	1.7 ± 0.8	3.4 ± 0.1*
Liver weight/body weight (%)	4.7 ± 1.3	8.6 ± 1.7*
Hepatic lipids (mg/g)		
Triglyceride	97 ± 81	235 ± 75*
Diacylglyceride	1.2 ± 0.2	3.0 ± 1.3*
Cholesterol ester	0.8 ± 0.6	108 ± 38*
Cholesterol	0.48 ± 0.23	1.22 ± 0.6*
Free fatty acid	3.1 ± 0.6	3.7 ± 1.5
Plasma levels, fasting		
ALT (U/L)	88 ± 83	319 ± 111*
Cholesterol (mg/dl)	86 ± 49	262 ± 66*
Triglyceride (mg/dl)	44 ± 12	35 ± 14
Glucose (mg/dl)	239 ± 35	290 ± 44*
Insulin (ng/ml)	2.78 ± 1.77	3.26 ± 2.49
Adiponectin (μg/ml)	5.2 ± 1.4	3.2 ± 0.8*
Hepatic mRNA analysis (relative expression)		
Nalp3	1 ± 0.5	1.8 ± 1.3
ASC	1 ± 0.6	1.5 ± 0.9
Caspase-1	1 ± 0.7	1.5 ± 1.5
Pannexin-1	1 ± 0.5	1.2 ± 0.7

*Indicates a comparison between HFHC and HF with a statistical significance of $P < 0.05$.

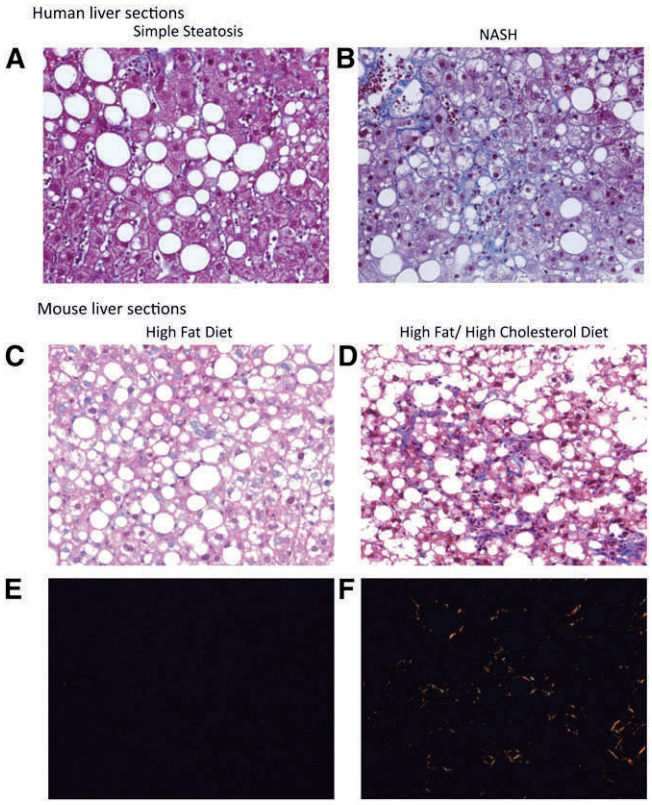

Fig. 1. A, B: Human specimens. Representative liver sections stained with Masson's trichrome from the patients included in this study with simple steatosis (A) or NASH (B). In patients with NASH the sections show moderate steatosis with a lobular inflammatory infiltrate and perisinusoidal ("chicken wire") fibrosis. In patients with simple steatosis, moderate steatosis is demonstrated with little/no inflammation and no fibrosis (×200 magnification). C–F: Mouse specimens. Representative liver sections stained with Masson's trichrome (C, D) or Sirius red (E, F, viewed with polarized light) from C57BL/6J mice fed either a HF diet or a HFHC diet for 30 weeks. Mice on a HFHC diet (D, F) developed severe steatosis with substantial inflammatory infiltrate and perisinusoidal, chicken wire fibrosis consistent with NASH. Mice on a HF diet (C, E) developed moderate steatosis with little inflammatory infiltrate and no fibrosis (simple steatosis) (×200 magnification).

(marked LD in Fig. 5) in healthy hepatocytes stained gray/brown with osmium either on electron microscopy or light microscopy (Fig. 5), the remnant lipid droplets of dead hepatocytes (marked by asterisks) that were surrounded by Kupffer cells did not stain with osmium, suggesting that they no longer contained triglyceride or cholesterol esters. Instead, they contained a granular precipitate and corresponded to the intensely birefringent droplets, including those exhibiting Maltese crosses, suggesting that they contained cholesterol in crystallized form. Furthermore, the Kupffer cells that aggregated around remnant lipid droplets had enlarged and become foam cells filled with a large number of much smaller lipid droplets which did not stain with osmium (Fig. 5C, E and supplementary Fig. IIB, F). The intense staining of the Kupffer cells with filipin and the lack of osmium staining suggests that these droplets contained free cholesterol, but not cholesterol esters, triglycerides, or free fatty acids. Taken together these findings suggest that Kupffer cells aggregate around remnant lipid droplets of dead hepatocytes that contain cholesterol crystals forming crown-like structures. Triglycerides and cholesterol esters within lipid droplets are hydrolyzed and resultant free fatty acids oxidized, but free cholesterol accumulates in activated Kupffer cells which turn into foam cells.

In contrast, mouse and human frozen liver sections with simple steatosis did not have any birefringent material and did not stain with filipin within hepatocyte lipid droplets (Fig. 2), suggesting absence of cholesterol crystals and unesterified cholesterol in simple steatosis. Although CD68-positive cells (Kupffer cells) were identified, they did not cluster around steatotic hepatocytes and did not stain with filipin. On electron microscopy, these Kupffer cells were not enlarged, did not contain lipid droplets, and did not aggregate around steatotic hepatocytes (supplementary Fig. II).

Hepatic mRNA levels of 4 genes associated with the NLRP3 inflammasome (Nalp3, ASC, Caspase-1, and Pannexin-1) were all greater in mice with NASH than in mice with simple steatosis, but did not reach statistical significance (Table 2).

DISCUSSION

Our results show that cholesterol crystals were present within steatotic hepatocytes in patients with NASH and in a mouse model of NASH induced by a HFHC diet, but not in patients or mice with simple steatosis. Enlarged Kupffer cells surrounded steatotic dead hepatocytes that included cholesterol crystals and appeared to process the remnant lipid droplets within these hepatocytes forming crown-like

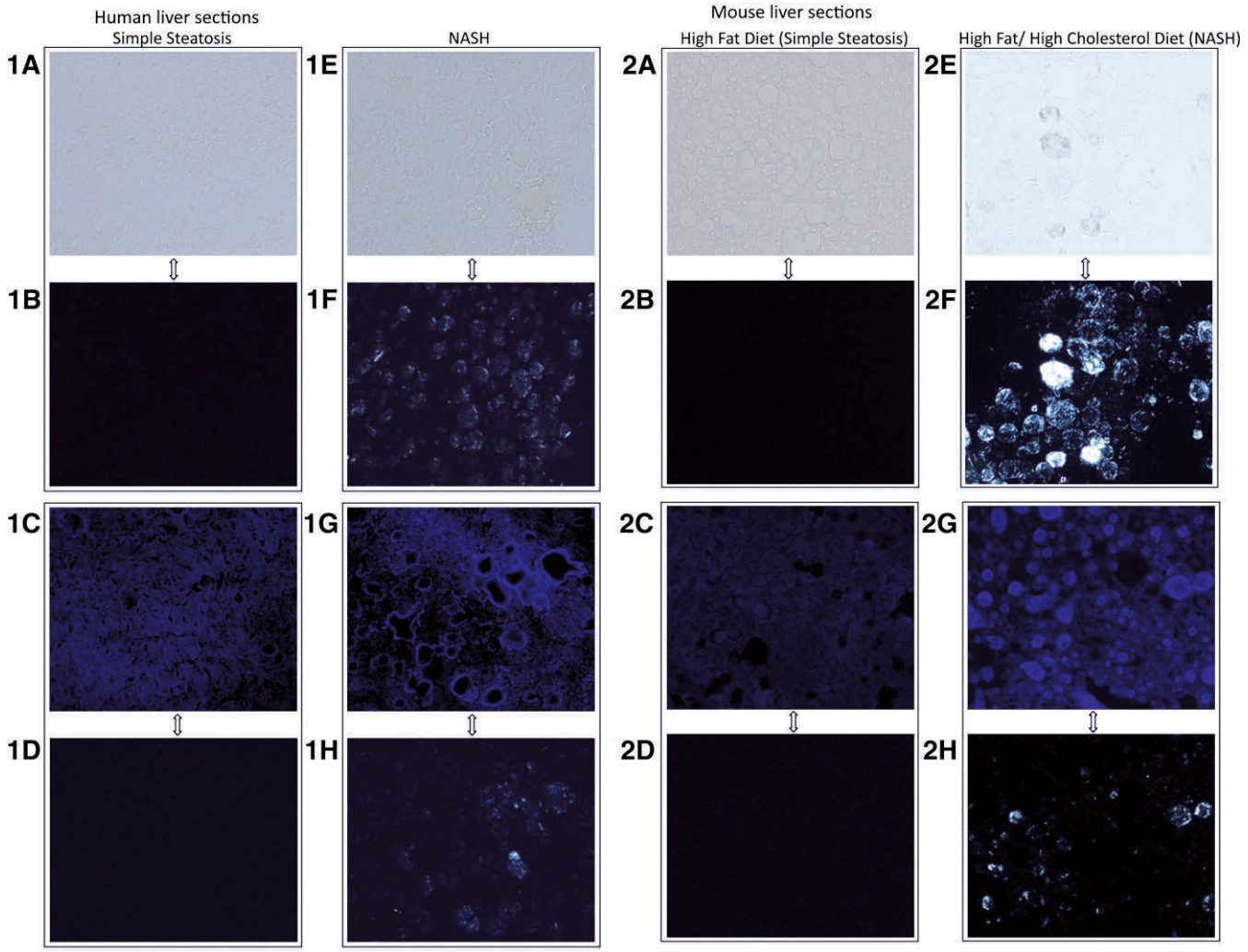

Fig. 2. Human (1A–H) and mouse (2A–H) frozen liver sections from livers with either simple steatosis (A–D) or NASH (E–H) (×200 magnification). A, E: Bright field images (no stain). B, F: Sections (A) and (E) viewed with polarized light to show colocalization of lipid droplets with birefringence in NASH. C, G: Filipin stain (blue) for free cholesterol. D, H: Sections (C) and (G) viewed with polarized light to show colocalization of filipin staining and birefringence in NASH. Livers with NASH exhibited strongly birefringent crystals within a large proportion of lipid droplets when viewed under polarized light (F, H). Filipin, which stains free cholesterol, also stained prominently the same droplets that had birefringence in livers with NASH, suggesting that the birefringence was due to cholesterol crystals. In contrast, livers with simple steatosis (A–D) did not exhibit any birefringence under polarized light despite having multiple lipid droplets within hepatocytes as seen in the bright field image (A) and did not contain excessive free cholesterol [absence of blue stain in (C)].

structures similar to those recently described in inflamed visceral adipose tissue (20, 21). This lipid scavenging resulted in profound accumulation of cholesterol within small droplets in markedly enlarged activated Kupffer cells that took the appearance of lipid-laden foam cells. This process may represent an important pathogenetic mechanism in NASH because exposure of macrophages to excess free cholesterol and cholesterol crystals has been shown to lead to their activation (13).

Several recent lines of evidence suggest that dietary cholesterol plays an important role in the pathogenesis of NASH. We reported that addition of dietary cholesterol to a high-fat diet causes progression from simple steatosis to steatohepatitis in C57BL/6J mice (16). Addition of dietary cholesterol to a high-fat high-carbohydrate diabetogenic diet led to increased hepatic steatosis, inflammation, and fibrosis in LDL receptor-deficient mice (8). Addition of cholesterol to the diet of *Alms1* mutant (*foz/foz*) mice, which are obese and insulin resistant, led to accumulation of hepatic free cholesterol, hepatocyte apoptosis, macrophage recruitment, and liver fibrosis (9). Administration of a liver X receptor agonist to hyperlipidemic mice with NASH decreases hepatic accumulation of free cholesterol and increases hepatic accumulation of triglyceride, accompanied by a decrease in hepatic inflammation (22). Thus, in that experimental model, the effects of triglycerides (responsible for most of the observed "steatosis") were dissociated from the effects of free cholesterol (potentially responsible for the inflammation) (22).

How exposure of the liver to excess cholesterol might promote the progression of simple steatosis to steatohepatitis remains unclear. Our results suggest that a critical early step might be crystallization of cholesterol within fatty hepatocytes. We identified a striking association between

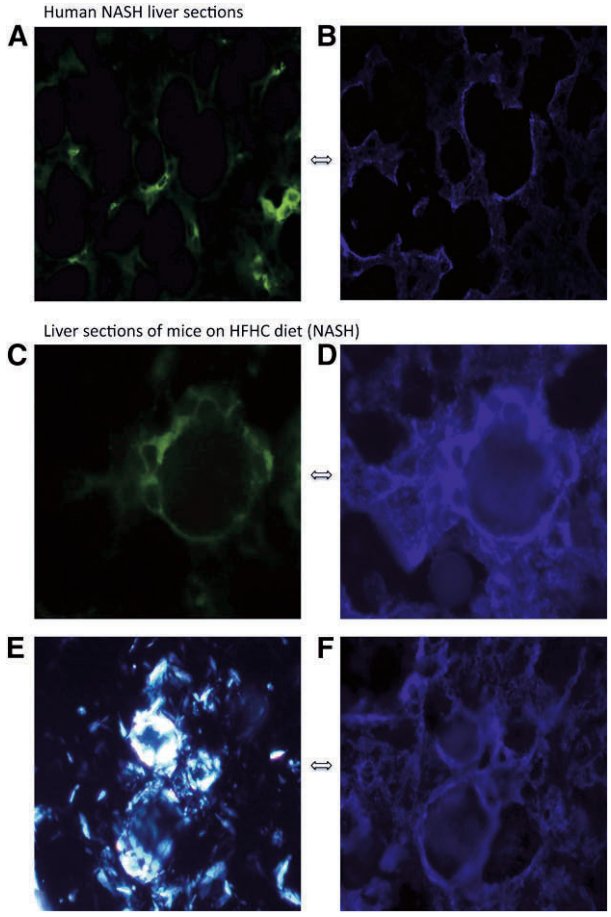

Fig. 3. Human (A, B) and mouse (C–F) liver sections with NASH stained with anti-CD68 antibody [stains green and identifies Kupffer cells (macrophages) (A, C)] or filipin [(B, D, F) stains blue and identifies unesterified cholesterol] and viewed using a fluorescent microscope (A–D, F) or viewed with polarized light (E) to identify birefringent crystals. Kupffer cells (green) surround hepatocytes and stain very strongly for free cholesterol (blue) as shown by the similarity in the blue and green patterns in (A) and (B) (which are the same human liver section) or (C) and (D) (which are the same mouse liver section). The strongly birefringent crystalline material (E) is shown to colocalize with free cholesterol in (F) by the similarity of the patterns of (E) and (F) which are the same mouse liver section. Taken together these sections suggest that in NASH, Kupffer cells aggregate around hepatocytes that contain cholesterol crystals and accumulate cholesterol (×800 magnification).

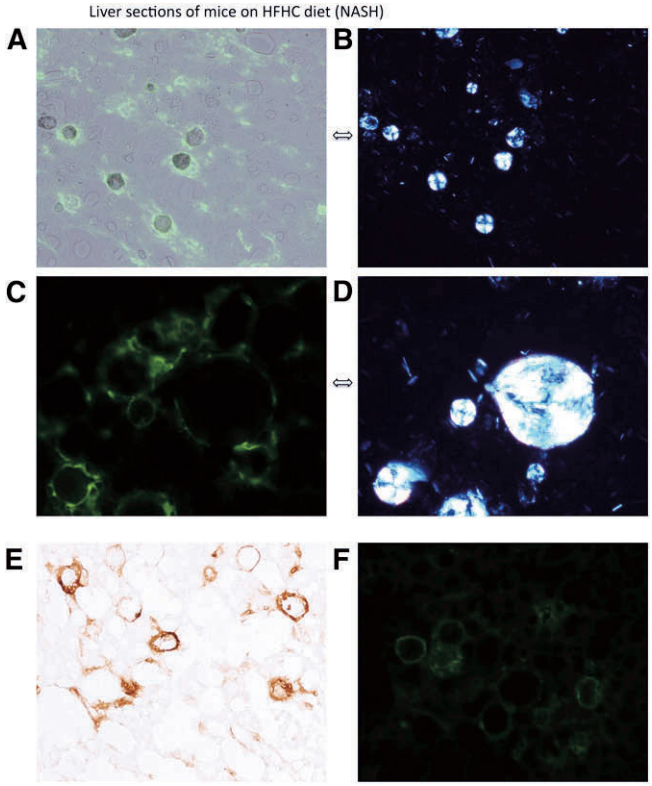

Fig. 4. Liver sections of mice on a HFHC diet (NASH) stained with anti-CD68 [stains green and identifies Kupffer cells (A–D)] or anti-CD11b [stains brown and identifies activated Kupffer cells (E)] or anti-TNFα [stains green and identifies activated Kupffer cells (F)] and viewed with fluorescent microscopy (A, C, F), polarized light (B, D) to identify birefringent crystals, or bright field microscopy (E). Pairs (A, B) and (C, D) are photomicrographs of the same liver section viewed with either fluorescent or polarized light showing Kupffer cells (green) aggregating around intensely birefringent lipid droplets containing cholesterol in crystallized form that creates a Maltese cross appearance. CD11b stain in panel (E) and TNFα staining in panel (F) suggest that the Kupffer cells are activated and show morphology very similar to previously described crown-like structures in inflamed visceral adipose tissue. We confirmed that TNFα colocalizes on CD68-positive cells (Kupffer cells) in supplementary Fig. IV [(A, B, E, F) are ×200 magnification; (C, D) are ×800 magnification].

the presence of cholesterol crystals within hepatocyte lipid droplets and the presence of NASH versus simple steatosis in both humans and mice. Although hepatocyte lipid droplets were readily evident both in NASH and simple steatosis, cholesterol crystals were present only in the lipid droplets of livers with NASH but not in the lipid droplets of livers with simple steatosis.

Moreover, the steatotic hepatocytes with strong birefringence were associated with striking changes in surrounding Kupffer cells, suggesting that the cholesterol crystals were more than innocent bystanders. Only steatotic dead hepatocytes that contained cholesterol crystals were encircled by enlarged Kupffer cells, which were transformed into activated foam cells containing many lipid droplets composed of free cholesterol (filipin positive), but no fatty acids, triglycerides, or cholesterol esters (osmium negative). The aggregates of foam cells encircling lipid-laden hepatocyte remnants formed crown-like structures similar to those recently described in inflamed visceral adipose tissue (20, 21). The enveloping Kupffer cells often appeared to be directly abutting on lipid cores which lacked evident hepatocyte cytoplasm. The enlarged Kupffer cells aggregated around dead, strongly birefringent hepatocytes, forming crown-like structures, similar to the encirclement of dead adipocytes by macrophages in inflamed visceral adipose tissue (20, 21). (In those studies, however, no connection was suggested with cholesterol or cholesterol crystals.) Those livers with such activated Kupffer cells manifested the inflammation and fibrosis that distinguish NASH from simple steatosis.

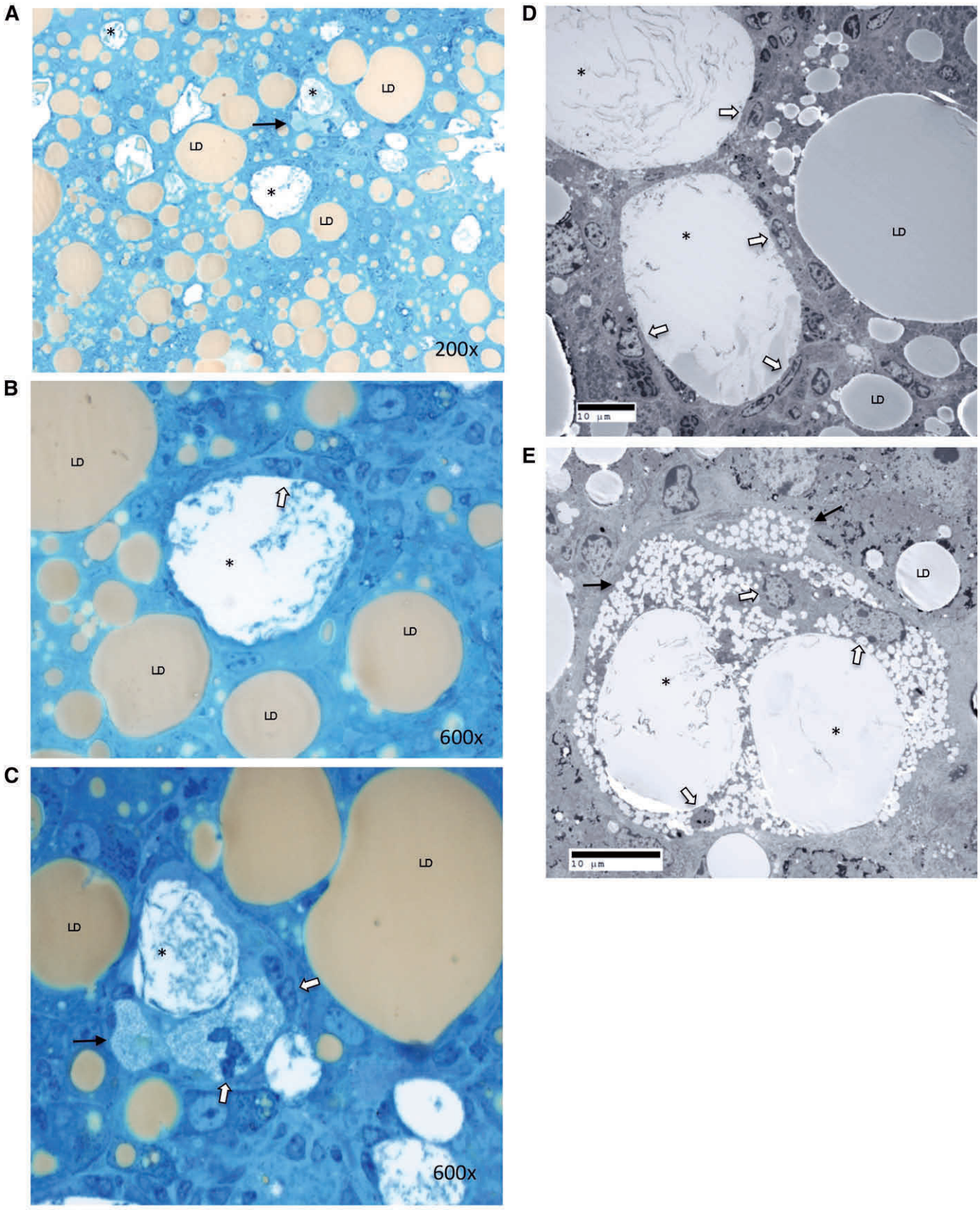
Liver sections of mice on HFHC diet (NASH)
A
B
C
D
E
LD
*
200x
600x
600x
10 µm
10 µm

Our interpretation of these findings is that the Kupffer cells scavenged the free cholesterol (including crystals), cholesterol esters, and triglycerides from the remnant large lipid droplets of dead hepatocytes. The Kupffer cells then presumably hydrolyzed the cholesterol esters and triglycerides followed by oxidation of the released fatty acids, accounting for the absence of osmium staining in the droplets within the Kupffer cells. Free cholesterol, whether derived from cholesterol crystals, hydrolysis of cholesterol esters, or uptake of unesterified cholesterol, could not be further metabolized, and accumulated in the smaller droplets within the enlarged Kupffer cells. Those Kupffer cells ingesting cholesterol crystals metamorphosed into activated foam cells, which in turn activated the inflammatory and fibrotic pathways that cause NAFLD to progress into NASH. Exposure of macrophages to excess free cholesterol and cholesterol crystals has been shown to lead to their activation (13). Future studies that directly modulate cholesterol crystallization, macrophage aggregation, or inflammasome activation will be required to prove this proposed sequence of events.

In a series of excellent recent papers, Dutch investigators identified foamy Kupffer cells in the liver of LDL receptor-deficient mice fed a high-fat high-cholesterol diet (22–26). However, they postulated that this cholesterol was derived from uptake of modified circulating lipoproteins by scavenger receptors on the Kupffer cells (24, 25). While this process may also be occurring, our results suggest that processing of remnant lipid droplets from dead steatotic hepatocytes represents an important mechanism by which macrophages acquire cholesterol.

There are striking and potentially informative similarities between the hepatic crown-like structures we observed in NASH and the crown-like structures recently described in inflamed adipose tissue (20, 21). In the latter, dead adipocytes were shown to be surrounded by macrophages that "scavenged" the residual adipocyte lipid droplet and ultimately formed multinucleate giant cells, a hallmark of chronic inflammation. We observed the same enveloping and processing of dead steatotic hepatocytes by Kupffer cells in NASH. However, we additionally observed that the Kupffer cells became loaded with cholesterol-containing droplets (foam cells) which were not described in the case of adipose tissue macrophages. We believe that this is due to the high concentration of cholesterol (free and esterified) in the hepatic lipid droplets.

Inflammasomes are multiprotein complexes which, once activated, promote the maturation and release of pro-inflammatory interleukins via activation of caspase-1. Recent studies have suggested that activation of the NLRP3 inflammasome in hepatic Kupffer cells is an important trigger for inflammation in NASH and may therefore contribute to the progression from simple steatosis to NASH (27–29). However, what may be activating the inflammasome in NASH was unclear. In the setting of atherosclerosis, cholesterol crystals have been shown recently to activate the NLRP3 inflammasome in macrophages (13). Given these findings and our demonstration of cholesterol crystal-containing lipid being processed by Kupffer cells in NASH, it is tempting to speculate that cholesterol crystals activate the NLRP3 inflammasome in Kupffer cells triggering an inflammatory response and promoting progression from simple steatosis to NASH. We identified increased expression of NLRP3 genes in our mice with NASH compared with the mice with simple steatosis, but the difference was not statistically significant. The lack of statistical significance may not be surprising considering that NLRP3 genes are expressed primarily by Kupffer cells, which constitute less than 10% of all liver cells. Future studies will be needed to specifically prove this hypothesis.

Our study is limited by the small number of patients studied and the fact that patients with NASH were not matched to those with simple steatosis with respect to diabetes, obesity, or insulin resistance. Future human studies with a larger sample size will be required to confirm the associations that we have described between hepatic cholesterol crystals and NASH, and to determine if these associations are independent of potential confounders such as diabetes, insulin resistance, and obesity.

Our results suggest that an important trigger for progression of simple steatosis to steatohepatitis (NASH) might be the accumulation of sufficient concentrations of free cholesterol within steatotic hepatocytes to cause crystallization of cholesterol. We identified a strong association between the presence of cholesterol crystals within hepatocyte lipid droplets, aggregation and activation of Kupffer cells in crown-like structures around such droplets, and the presence of NASH versus simple steatosis, in both humans and mice. Although hepatocyte lipid droplets were abundant in both NASH and simple steatosis, cholesterol crystals were observed only in the lipid droplets of livers with NASH. These associations need to be confirmed in larger numbers of human liver specimens and in additional animal models.

Fig. 5. Liver sections of mice on a HFHC diet (NASH) stained with osmium and methylene blue (A–C) or viewed with transmission electron microscopy (D, E). Osmium staining with methylene blue counterstaining readily identifies multiple crown-like structures because the remnant lipid droplet of the dead hepatocyte does not take up osmium (marked with asterisks) while all other normal lipid droplets (LD) in viable hepatocytes take up osmium and stain gray/brown. Higher magnification of two of the crown-like structures in panel (A) is shown in panels (B) and (C), demonstrating a granular precipitate within the remnant lipid droplets (marked with asterisks) that are surrounded by Kupffer cells (white arrows). Panel (C) shows that the Kupffer cells acquire multiple small non-osmium binding cholesterol droplets (black arrow) as processing of the remnant lipid droplet of the dead hepatocyte advances. Crown-like structures viewed by electron microscopy are shown in (D) and (E) again demonstrating multiple Kupffer cells (white arrows) surrounding and processing remnant lipid droplets (marked with asterisks) of dead hepatocytes. These remnant droplets do not take osmium (which is used in electron microscopy fixation) and are shown again to contain a granular precipitate in contrast to healthy hepatocyte lipid droplets (LD) that stain gray. In (E) the Kupffer cells have acquired multiple small cholesterol droplets (black arrows) turning into foam cells. The remnant lipid droplets of dead hepatocytes that do not stain with osmium correspond to the intensely birefringent droplets (Maltese crosses) seen by polarized light in Fig. 4B and D.

The potential causative role of these associations deserves further examination in interventional studies.

In memory of our teacher, colleague, and friend, Don J. Ostrow, who provided careful and insightful comments to our manuscript. We also acknowledge Deborah Jones for her expert assistance with electron microscopy.

REFERENCES

1. Browning, J. D., L. S. Szczepaniak, R. Dobbins, P. Nuremberg, J. D. Horton, J. C. Cohen, S. M. Grundy, and H. H. Hobbs. 2004. Prevalence of hepatic steatosis in an urban population in the United States: impact of ethnicity. *Hepatology.* **40:** 1387–1395.
2. Bellentani, S., G. Saccoccio, F. Masutti, L. S. Croce, G. Brandi, F. Sasso, G. Cristanini, and C. Tiribelli. 2000. Prevalence of and risk factors for hepatic steatosis in Northern Italy. *Ann. Intern. Med.* **132:** 112–117.
3. Williams, C. D., J. Stengel, M. I. Asike, D. M. Torres, J. Shaw, M. Contreras, C. L. Landt, and S. A. Harrison. 2011. Prevalence of nonalcoholic fatty liver disease and nonalcoholic steatohepatitis among a largely middle-aged population utilizing ultrasound and liver biopsy: a prospective study. *Gastroenterology.* **140:** 124–131.
4. Matteoni, C. A., Z. M. Younossi, T. Gramlich, N. Boparai, Y. C. Liu, and A. J. McCullough. 1999. Nonalcoholic fatty liver disease: a spectrum of clinical and pathological severity. *Gastroenterology.* **116:** 1413–1419.
5. Bugianesi, E., N. Leone, E. Vanni, G. Marchesini, F. Brunello, P. Carucci, A. Musso, P. De Paolis, L. Capussotti, M. Salizzoni, et al. 2002. Expanding the natural history of nonalcoholic steatohepatitis: from cryptogenic cirrhosis to hepatocellular carcinoma. *Gastroenterology.* **123:** 134–140.
6. Matsuzawa, N., T. Takamura, S. Kurita, H. Misu, T. Ota, H. Ando, M. Yokoyama, M. Honda, Y. Zen, Y. Nakanuma, et al. 2007. Lipid-induced oxidative stress causes steatohepatitis in mice fed an atherogenic diet. *Hepatology.* **46:** 1392–1403.
7. Zheng, S., L. Hoos, J. Cook, G. Tetzloff, H. Davis, Jr., M. van Heek, and J. J. Hwa. 2008. Ezetimibe improves high fat and cholesterol diet-induced non-alcoholic fatty liver disease in mice. *Eur. J. Pharmacol.* **584:** 118–124.
8. Subramanian, S., L. Goodspeed, S. A. Wang, J. Kim, L. Zeng, G. N. Ioannou, W. G. Haigh, M. M. Yeh, K. V. Kowdley, K. D. O'Brien, et al. 2011. Dietary cholesterol exacerbates hepatic steatosis and inflammation in obese LDL receptor-deficient mice. *J. Lipid Res.* **52:** 1626–1635.
9. Van Rooyen, D. M., C. Z. Larter, W. G. Haigh, M. M. Yeh, G. Ioannou, R. Kuver, S. P. Lee, N. C. Teoh, and G. C. Farrell. 2011. Hepatic free cholesterol accumulates in obese, diabetic mice and causes nonalcoholic steatohepatitis. *Gastroenterology.* **141:** 1393–1403.
10. Ioannou, G. N., O. B. Morrow, M. L. Connole, and S. P. Lee. 2009. Association between dietary nutrient composition and the incidence of cirrhosis or liver cancer in the United States population. *Hepatology.* **50:** 175–184.
11. Yoneda, M., K. Fujita, Y. Nozaki, H. Endo, H. Takahashi, K. Hosono, K. Suzuki, H. Mawatari, H. Kirikoshi, M. Inamori, et al. 2010. Efficacy of ezetimibe for the treatment of non-alcoholic steatohepatitis: an open-label, pilot study. *Hepatol. Res.* **40:** 613–621.
12. Park, H., T. Shima, K. Yamaguchi, H. Mitsuyoshi, M. Minami, K. Yasui, Y. Itoh, T. Yoshikawa, M. Fukui, G. Hasegawa, et al. 2011. Efficacy of long-term ezetimibe therapy in patients with nonalcoholic fatty liver disease. *J. Gastroenterol.* **46:** 101–107.
13. Duewell, P., H. Kono, K. J. Rayner, C. M. Sirois, G. Vladimer, F. G. Bauernfeind, G. S. Abela, L. Franchi, G. Nunez, M. Schnurr, et al. 2010. NLRP3 inflammasomes are required for atherogenesis and activated by cholesterol crystals. *Nature.* **464:** 1357–1361.
14. Di Bisceglie, A. M., K. G. Ishak, L. Rabin, and J. M. Hoeg. 1990. Cholesteryl ester storage disease: hepatopathology and effects of therapy with lovastatin. *Hepatology.* **11:** 764–772.
15. Kleiner, D. E., E. M. Brunt, M. Van Natta, C. Behling, M. J. Contos, O. W. Cummings, L. D. Ferrell, Y. C. Liu, M. S. Torbenson, A. Unalp-Arida, et al. 2005. Design and validation of a histological scoring system for nonalcoholic fatty liver disease. *Hepatology.* **41:** 1313–1321.
16. Savard, C., E. V. Tartaglione, R. Kuver, W. Geoffrey Haigh, G. C. Farrell, S. Subramanian, A. Chait, M. M. Yeh, L. S. Quinn, and G. N. Ioannou. 2013. Synergistic interaction of dietary cholesterol and dietary fat in inducing experimental steatohepatitis. *Hepatology.* **57:** 81–92.
17. Rudolf, M., and C. A. Curcio. 2009. Esterified cholesterol is highly localized to Bruch's membrane, as revealed by lipid histochemistry in wholemounts of human choroid. *J. Histochem. Cytochem.* **57:** 731–739.
18. Folch, J., M. Lees, and G. H. Sloane Stanley. 1957. A simple method for the isolation and purification of total lipides from animal tissues. *J. Biol. Chem.* **226:** 497–509.
19. Ganz, M., T. Csak, B. Nath, and G. Szabo. 2011. Lipopolysaccharide induces and activates the Nalp3 inflammasome in the liver. *World J. Gastroenterol.* **17:** 4772–4778.
20. Cinti, S., G. Mitchell, G. Barbatelli, I. Murano, E. Ceresi, E. Faloia, S. Wang, M. Fortier, A. S. Greenberg, and M. S. Obin. 2005. Adipocyte death defines macrophage localization and function in adipose tissue of obese mice and humans. *J. Lipid Res.* **46:** 2347–2355.
21. Strissel, K. J., Z. Stancheva, H. Miyoshi, J. W. Perfield 2nd, J. DeFuria, Z. Jick, A. S. Greenberg, and M. S. Obin. 2007. Adipocyte death, adipose tissue remodeling, and obesity complications. *Diabetes.* **56:** 2910–2918.
22. Wouters, K., M. van Bilsen, P. J. van Gorp, V. Bieghs, D. Lutjohann, A. Kerksiek, B. Staels, M. H. Hofker, and R. Shiri-Sverdlov. 2010. Intrahepatic cholesterol influences progression, inhibition and reversal of non-alcoholic steatohepatitis in hyperlipidemic mice. *FEBS Lett.* **584:** 1001–1005.
23. Wouters, K., P. J. van Gorp, V. Bieghs, M. J. Gijbels, H. Duimel, D. Lutjohann, A. Kerksiek, R. van Kruchten, N. Maeda, B. Staels, et al. 2008. Dietary cholesterol, rather than liver steatosis, leads to hepatic inflammation in hyperlipidemic mouse models of nonalcoholic steatohepatitis. *Hepatology.* **48:** 474–486.
24. Bieghs, V., F. Verheyen, P. J. van Gorp, T. Hendrikx, K. Wouters, D. Lutjohann, M. J. Gijbels, M. Febbraio, C. J. Binder, M. H. Hofker, et al. 2012. Internalization of modified lipids by CD36 and SR-A leads to hepatic inflammation and lysosomal cholesterol storage in Kupffer cells. *PLoS ONE.* **7:** e34378.
25. Bieghs, V., K. Wouters, P. J. van Gorp, M. J. Gijbels, M. P. de Winther, C. J. Binder, D. Lutjohann, M. Febbraio, K. J. Moore, M. van Bilsen, M. H., et al. 2010. Role of scavenger receptor A and CD36 in diet-induced nonalcoholic steatohepatitis in hyperlipidemic mice. *Gastroenterology.* **138:** 2477–2486.
26. Bieghs, V., T. Hendrikx, P. J. van Gorp, F. Verheyen, Y. D. Guichot, S. M. Walenbergh, M. Gijbels, S. S. Rensen, A. Bast, J. Plat, et al. 2013. The cholesterol derivative 27-hydroxycholesterol reduces steatohepatitis in mice. *Gastroenterology.* **144:** 167–178.
27. Dixon, L. J., M. Berk, S. Thapaliya, B. G. Papouchado, and A. E. Feldstein. 2012. Caspase-1-mediated regulation of fibrogenesis in diet-induced steatohepatitis. *Lab. Invest.* **92:** 713–723.
28. Walenbergh, S., T. Hendrikx, V. Bieghs, P. J. Van Gorp, M. M. Steinbusch, and R. Shiri-Sverdlov. 2012. The inflammasome as a novel target for the detection and treatment of non-alcoholic steatohepatitis (Abstract #1450 in The Liver Meeting. Boston, MA, November 9–13, 2012).
29. Wree, A., C. L. Johnson, A. Eguchi, H. M. Hoffman, and A. Feldstein. 2012. Constitutive mutant NLRP3 expression in myeloid cells leads to spontaneous liver inflammation and fibrosis (Abstract #1946 in The Liver Meeting. Boston, MA, November 9–13, 2012).